Laser-induced modification of a structured continuum observed in ionization and harmonic generation

O. Faucher,[1] Y. L. Shao,[1] D. Charalambidis,[1,2] and C. Fotakis[1,2]
[1]*Foundation for Research and Technology, Hellas, Institute of Electronic Structure and Laser, P.O. Box 1527, Heraklion 71110, Crete, Greece*
[2]*Department of Physics, University of Crete, Crete, Greece*
(Received 27 December 1993)

Experimental investigations of the laser-induced continuum structure in the vicinity of autoionizing states (AIS's) of Ca are reported for both ionization and third-harmonic generation. The shape of the induced structures is shown to be strongly affected by the presence of the AIS's, as well as exhibiting a detuning- and laser-intensity-dependent transition from a window resonance dip to a peak. The observed modification of the continuum is discussed in terms of interfering excitation channels.

PACS number(s): 32.80.Wr, 32.80.Dz, 42.65.Ky

I. INTRODUCTION

A discrete state embedded in a continuum provides an appropriate scheme for the observation of a quantum-mechanical interference. That is the interference between two outgoing waves resulting from the direct decay of the system into the continuum, and its decay through the embedded discrete state. Such interference effects can be traced back to the elastic resonant scattering of particles on nuclei [1]; autoionization is the best known phenomenon of the same nature in atomic and molecular physics [2]. It is now known that the embedded state does not necessarily have to be an autoionizing state (AIS) of the system, but can also be induced by means of a strong electromagnetic wave that couples a bound excited state with the continuum. The full analogy of this scheme to autoionization has been pointed out by Dai *et al.* [3] and lies on the coupling of two bound states to each other and to the same continuum. In addition to the value of such effects as a demonstration of quantum-mechanical interference, a destructive interference minimum caused either through autoionization or coherent interactions breaks the symmetry between absorption and stimulated emission. Therefore this has been considered a promising candidate for amplification without inversion of population [4,5]. Inversionless amplification or lasing is subsequently more favorable for short-wavelength lasing systems.

The dressing of a continuum, by embedding a bound state, through an external electromagnetic (EM) field, and the observation of the induced "autoionizing like" structure via a second EM field has been a challenging experimental problem for the last 15 years [6–13]. Despite rather numerous theoretical papers referring to this subject (for instance, see Ref. [14] and references therein), only few experimental attempts have been able to demonstrate laser-induced continuum structures (LICS's), as exhibiting some degree of asymmetry and thus manifesting the interference character of the effect.

In two recent letters [15,16] we have reported the observation of LICS in the structured continuum of atomic Ca. The modification of doubly excited autoionizing states leads to the observation of interference features in the multiphoton ionization (MPI) and third-harmonic generation (THG) spectra. The shape of these features is strongly dependent on the laser power densities and detunings. The present work is a more detailed presentation of these results and reports additional and more recent experimental observations related to the subject under investigation. It includes results from two different experimental environments, namely those of simultaneous ionization and third-harmonic generation measurements in a heat pipe, as well as ionization in a low-pressure Ca effusive beam. It further reports about ac Stark splitting caused by the single-photon coupling of bound with autoionizing states, and discusses its role in the laser-induced structure observed in the vicinity of AIS's. Finally we present results recorded with different laser polarizations, in which bound and autoionizing states can be decoupled, demonstrating their role in the effects observed.

II. EXPERIMENTAL SETUP

Two types of experiments have been performed: (a) High-atomic-density experiments in a heat pipe, and (b) low-atomic-density experiments in an effusive beam. The setup is shown in Fig. 1. In both studies the optical arrangement was the same, consisting of two excimer-pumped dye lasers with 12-ns pulse durations. The two laser beams were appropriately delayed as to ensure optimum temporal overlapping of the pulses, combined with a dichroic beam splitter, and consequently focused in the interaction Ca vapor region via a 30-cm focal length achromatic lens.

The heat pipe oven has been operated at 900°C, resulting in a 5-mbar vapor pressure. Contamination of the windows was avoided through water cooling and the introduction of 15 mbar of He buffer gas. A biased electrode was placed in the heat-pipe oven for the collection of the ions produced in the interaction volume. A 25-cm vacuum ultraviolet (vuv) monochromator was connected to the heat-pipe LiF exit window. This was employed for

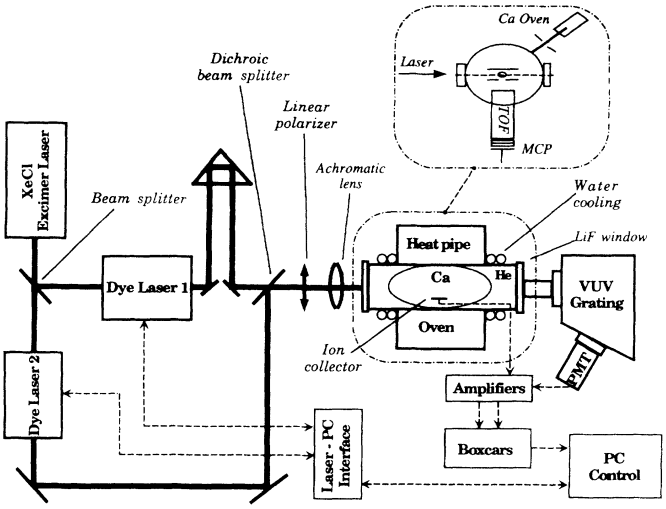

FIG. 1. Experimental setup. In the effusive beam experiments the heat pipe has been replaced by a vacuum chamber connected with a Ca oven shown in the inset.

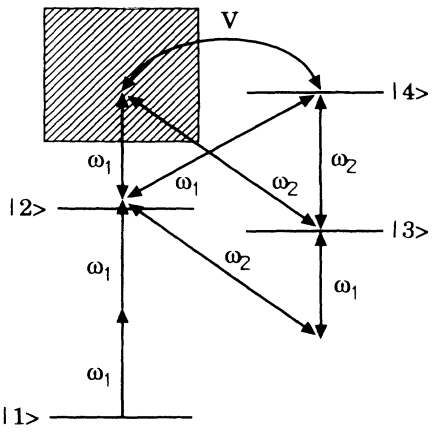

FIG. 2. Coupling scheme.

the separation of the third-harmonic radiation, produced in the heat pipe, from the two laser beams. The vuv radiation was detected with a solar-blind photomultiplier tube (PMT). An alumina filter was placed at the entrance of the PMT in order to reduce the background signal originating from scattered light of the two laser beams.

For the effusive beam experiment the heat pipe was exchanged with a vacuum chamber, as shown in the inset of Fig. 1. A 10^{-6}-mbar background pressure was kept via a turbo molecular pump. The Ca atoms were introduced in the interaction region in the form of an effusive beam, produced by employing a resistor-heated oven at a temperature of 500 °C. The Ca vapor number density in the interaction region was estimated to be 10^8 atoms/cm^3. The atomic and laser beams intersected each other at right angles. Ions produced during the laser–atomic-beam interaction were extracted perpendicularly to the direction of the laser and effusive beam with a static field. They were further mass analyzed by means of a time-of-flight mass spectrometer, and detected with a tandem multichannel plate detector.

All signals (MPI and THG) have been amplified and integrated on a shot-to-shot basis by a two-channel boxcar integrator. Each point of the recorded spectra was the average of 20 laser pulses. The boxcar outputs were digitized and stored in a microcomputer, which was also used to control the scanning and the triggering of the lasers.

III. RESULTS

The LICS scheme under investigation is illustrated in Fig. 2. It involves the three-photon excitation ($3\omega_1$) of the autoionizing state $|4\rangle$ (AIS) and the single-photon coupling (ω_2) of the bound state $|3\rangle$ to the vicinity of the $|4\rangle$ AIS. This scheme is more complicated than the conventional LICS scheme, where the two bound states are directly coupled to the smooth continuum. In the present scheme the decay of both bound states in the continuum is achieved through the autoionization processes depicted in Fig. 2. The bound-bound coupling through the continuum consists now of two Raman processes. One, being nonresonant, has a pole in the continuum, to which all allowed continuum and discrete states contribute; and the other is resonant with the $|4\rangle$ AIS. The latter is the dominant one in the present case. In addition a near-two-photon resonance condition ($2\omega_2$) is always fulfilled for the bound state $|2\rangle$.

The autoionizing states that have been investigated in this study are the $3d4f\,{}^1P_1$, ${}^3P_1$, and ${}^3D_1$ doubly excited states. The bound states coupled to the continuum have been the $4s6s\,{}^1S_0$ and $4p^2\,{}^1D_2$ states. The relevant energy levels and couplings are depicted in the inset of Fig. 3. In this scheme it happens that the $4s4d\,{}^1D_2$ state is near-

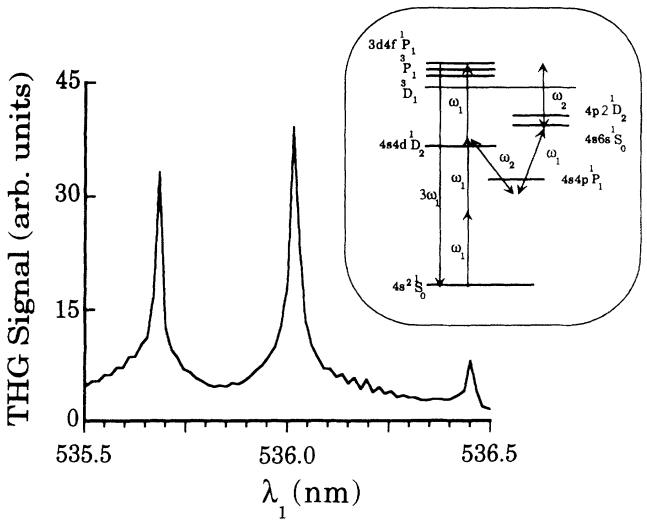

FIG. 3. One-color THG spectrum depicting the three autoionizing resonances $3d4f\,{}^1P_1$, ${}^3P_1$, and ${}^3D_1$. The central peak incorporates the unresolved two-photon resonance with the $4s4d\,{}^1D_2$ state (accidental double resonance). Inset: the essential atomic level diagram including the most relevant couplings.

two-photon resonant ($2\omega_1$) with the ground state, so that the dominant bound-bound couplings of the LICS process are the two-photon Raman processes, coupling the $4s4d\ ^1D_2$ with $4s6s\ ^1S_0$ or $4p^2\ ^1D_2$ state. In particular when the $3d4f\ ^3P_1$ (AIS) is three-photon resonant ($3\omega_1$), the two-photon step is only 0.5 cm^{-1} detuned from $4s4d\ ^1D_2$ state, thus leading to a double resonance.

In all the experimental runs the total ionization has been measured. This includes, besides the ionization channels of the LICS scheme, the incoherent ionization channel of state $|3\rangle$ through ω_1, and states $|1\rangle$ or $|2\rangle$ through ω_2 (or a combination of ω_2 and ω_1). An additional incoherent channel ionizes the $4p^2\ ^1D_2$ state through ω_2 and leads to an f outgoing wave. Results obtained with both (a) heat-pipe and (b) effusive beam arrangements will be presented. These results will be discussed in Sec. IV.

A. Heat-pipe spectra

In the heat-pipe arrangement third-harmonic generation ($\omega_3=3\omega_1$) has been measured simultaneously with ionization. Both laser beams had the same linear polarization.

A third-harmonic spectrum produced by laser I is shown in Fig. 3. The left and right peaks correspond to the three-photon excitation of the ^1P and ^3D AIS's, respectively. The peak in the center originates from the unresolved three-photon excitation of the ^3P AIS and the two-photon resonant three-photon ionization via the $4s4d\ ^1D_2$ state. The singlet-triplet couplings observed reflect the strong electron-electron correlation in Ca.

Keeping the wavelength of laser I fixed in order to match the excitation of the ^1P AIS, a second laser beam has been introduced and tuned as to couple this state with the $4s6s\ ^1P_1$ and $4p^2\ ^1D_2$ bound states. THG and MPI spectra are depicted in Fig. 4. The two shortest-wavelength dips are laser-induced structures corresponding to these couplings. The presence of field ω_2 intro-

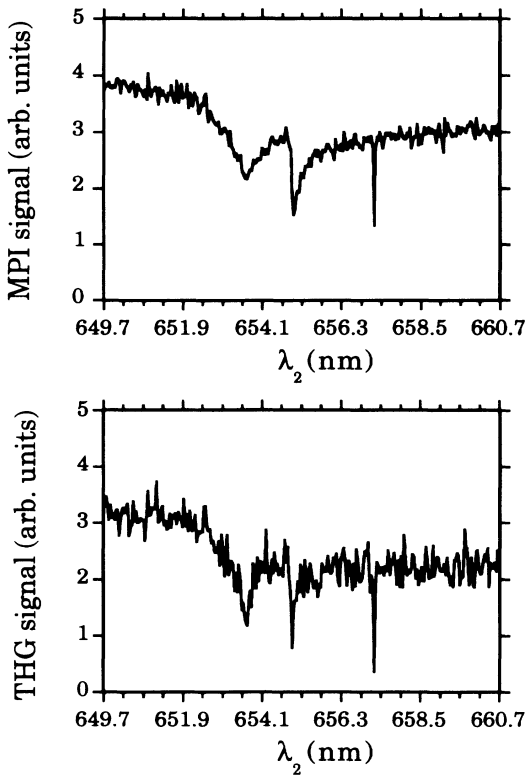

FIG. 4. Two-color THG and MPI spectra observed in the heat-pipe experiments. ω_1 is kept fixed to fulfill the three-photon resonant condition with the $3d4f\ ^1P_1$ AIS, whereas ω_2 is scanned. The first two dips are LICS's corresponding to the single-photon coupling of the AIS with the $4s6s\ ^1S_0$ and $4p^2\ ^1D_2$, respectively. The third dip reflects the ground-state depletion due to single-photon resonance with the $4s4p\ ^3P_1$ bound state (see text).

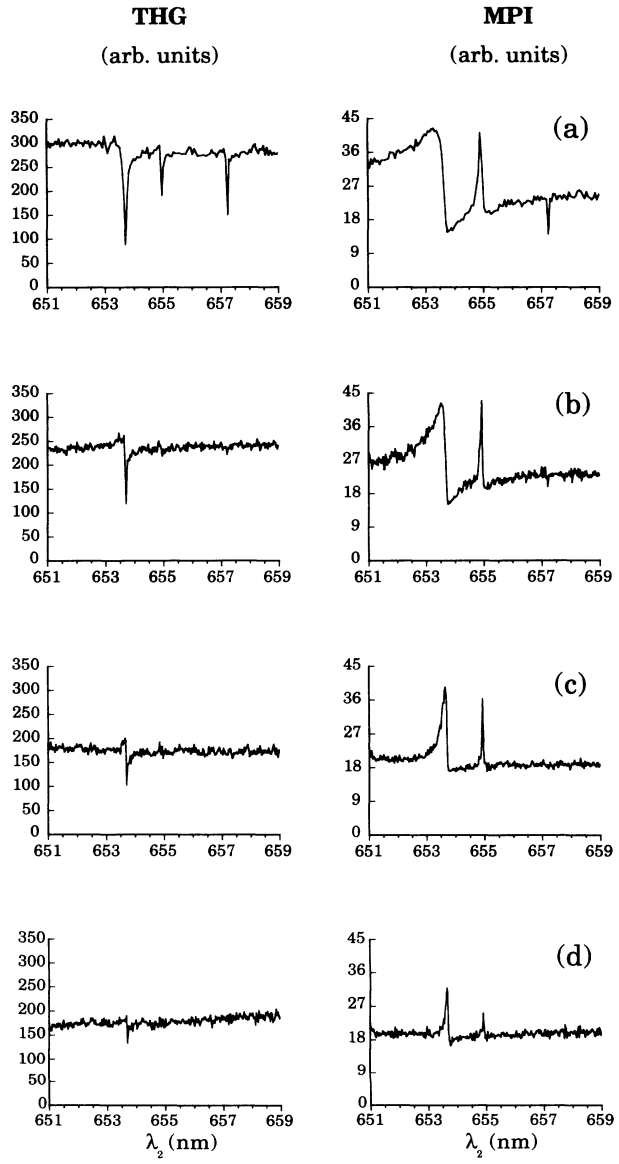

FIG. 5. Two-color THG and MPI spectra dependence on the intensity of the laser field ω_2. λ_1 is fixed as to match the three-photon resonance with the $3d4f\ ^1P_1$ AIS.

duces new coherent excitation channels. Their interference, which in this case is destructive, modifies the transitions involving the $^1P_1$ AIS. A more detailed discussion concerning these interferences follows in Sec. IV. The third dip of the spectra is due to the population depletion through the accidental one-photon resonant coupling of the ground with the $4s4p\ ^3P_1$ state at 657.4 nm. However, this feature is not pertinent to the effects under investigation.

Two similar LICS-related dips have been observed for the $^3P_1$ and $^3D_1$ AIS's (Ref. 15) as well as for the $4s5s\ ^1S_0$ bound state [16], the latter being single-photon coupled to the continuum. In all these cases ω_2 was tuned so as to match the energy balance condition for the laser-induced continuum structure:

$$3\hbar\omega_1 + E_{|1\rangle} = \hbar\omega_2 + E_{|3\rangle} \cong E_{|4\rangle} \ .$$

The shape of the induced structures is found to depend strongly on the laser intensities and spatial overlapping of the two laser beams. The laser intensity dependence for both MPI and THG spectra is shown in Figs. 5 and 6.

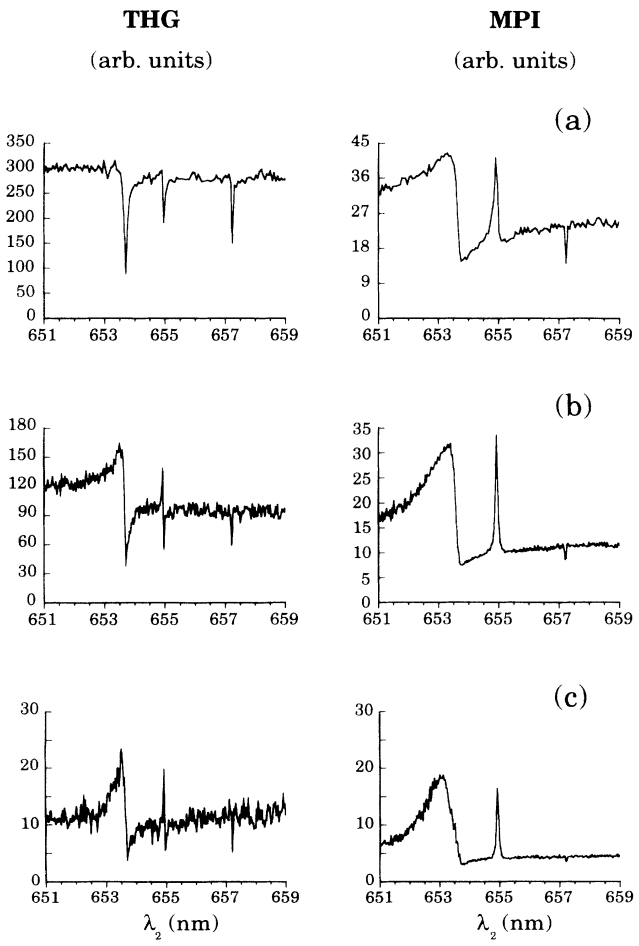

FIG. 6. Two-color THG and MPI spectra dependence on the intensity of the laser field ω_1.

The spectra of Fig. 5 have been recorded at constant intensity at the focus $I_1 = 21\times10^9$ W/cm^2 (laser I), while intensity I_2 (laser II) was 8×10^9 W/cm^2 (a), 4.5×10^9 W/cm^2 (b), 2.25×10^9 W/cm^2 (c), and 0.6×10^9 W/cm^2 (d). In Fig. 6 spectra observed with constant intensity $I_2 = 8\times10^9$ W/cm^2 and different intensity $I_1 = 21\times10^9$ W/cm^2 (a), 10.5×10^9 W/cm^2 (b), and 4.5×10^9 W/cm^2 (c) are shown. Varying I_2 (Fig. 5), the shape of the features in THG does not change significantly. The width and amplitude of the induced structure decreases, as expected, as the power density of laser II decreases. Variation of I_1 (Fig. 6) dramatically transforms the shape of the induced structure from a dip (window resonance) (a) to an asymmetric "Fano" type of profile exhibiting a maximum and a minimum (b), and further to a less asymmetric peak (c) as I_1 decreases. The structures observed in the MPI spectra in both figures exhibit decreasing width and asymmetry as I_1 or I_2 drops. This variable shape, controllable through the laser intensity, can also be the result of the detuning of $3\omega_1$ from the AIS, as will be shown and discussed in Secs. III B and IV.

In general, the presence of the THG complicates the interpretation of the MPI spectra. This is because reabsorption of the THG radiation opens additional ionization channels. Indeed, one could interpret the first two dips in the MPI spectrum of Fig. 4 as the result of the single harmonic photon ionization of the ground state. It is clear that the ionization spectrum would then follow the profile of the THG. The THG minima in turn may not be a LICS feature, but simply be due to the phase mismatch induced by laser II. In order to resolve this, experiments have been performed in a Ca effusive beam, in which the atomic density has been kept low as to ensure practically no THG.

B. Effusive beam spectra

MPI spectra, produced in the effusive Ca beam, have also been recorded as a function of ω_2, with $3\omega_1$ being resonant with the $^1P_1$ AIS. These spectra demonstrated clearly that the dips, observed in the heat-pipe arrangement, can be reproduced in an environment in which THG is absent.

The observed laser-induced structures have a strong shape dependence on the detuning $\Delta_1 = E_{|4\rangle} - 3\hbar\omega_1$. In Fig. 7, the window resonances (dip) which appear at near-zero detuning change to peaks with reversed asymmetry for positive and negative detunings. The larger the detuning, the narrower and more symmetric the laser-induced peaks become.

The dependence of the MPI spectra on I_1 and I_2 for small Δ_1 is similar to that of the heat-pipe spectra shown in Figs. 5 and 6. In these spectra, $3\omega_1$ is also slightly detuned from the AIS. Indeed, they have been recorded for optimum phase matching; that is, when $3\omega_1$ is slightly detuned from the $^1P_1$ AIS, where the medium becomes negatively dispersive as required by the focused geometry employed [17]. It is worth noting that in the effusive beam measurements it was not possible to change the dips to peaks by varying the laser power densities for zero detuning. The laser-induced dips are due to the presence

of the AIS. A verification of the above has been attempted by employing different polarization combinations of the two laser fields. Due to angular momentum conservation, states can selectively contribute to the process. These results are depicted in Fig. 8. While for linearly polarized beams with parallel polarizations the spectra show two laser-induced dips [Fig. 8(a)], for crossed polarizations the dip originating from the coupling of the $4s6s\ ^1S_0$ state disappears [Fig. 8(b)]. Since the ground state has a total angular momentum of $J=0$, crossed polarizations require an $M_J=\pm 1$ level of the excited bound state to be coupled with ω_2. Thus the total angular momentum of the bound state has to be $J\neq 0$, which explains why the $^1S_0$ resonance has been switched off. When laser I is circularly polarized, the $^1P_1$ AIS state cannot be coupled to the ground state, since three-photon absorption requires a $J=3$ ($M_J=+3$ or -3) final state. For this reason only $4p^2\,^1D_2$ ($M_J=\pm 2$) can be coupled with ω_2 to the $J=3$ continuum. Thus the LICS due to the $4s6s\ ^1S_0$ is again switched off, but in addition the AIS is decoupled. As a result of the latter, the dip due to the $4p^2\,^1D_2$ state, observed with linear polarizations, has now turned to a peak [Fig. 8(c)]. This scheme is of course slightly different from that of Fig. 8(a) due to the coupling of only the $J=3$ continuum, and to the different M_J levels participating. Nevertheless, this is not expected to affect significantly the shape of the induced resonance. It is rather the decoupling of the AIS that changes the induced structure from a dip to a peak.

Up to now all LICS spectra have been recorded by keeping ω_1 fixed, and scanning the coupling frequency ω_2. In the following, spectra obtained by scanning ω_1 for several fixed values of ω_2, corresponding to the $^1P_1$ AIS coupled either to the $4s6s\ ^1S_0$ or $4p^2\,^1D_2$ states, will be presented. Figure 9(a) shows the three-photon excitation spectrum in the vicinity of the three AIS without field ω_2. In Figs. 9(b), 9(c), and 9(d) field ω_2 couples the $4s6s\ ^1S_0$ with the continuum and is 10.6, 60.4, and $-12.8\ \mathrm{cm}^{-1}$ detuned from the $^1P_1$ AIS, respectively. For all three detunings the laser-induced structures appear as peaks, with positions satisfying the energy balance condition for the LICS process. For zero detuning from the $^1P_1$ AIS through field ω_2 causes a splitting of the peak corresponding to the decay of the $^1P_1$ AIS, as depicted in Fig.

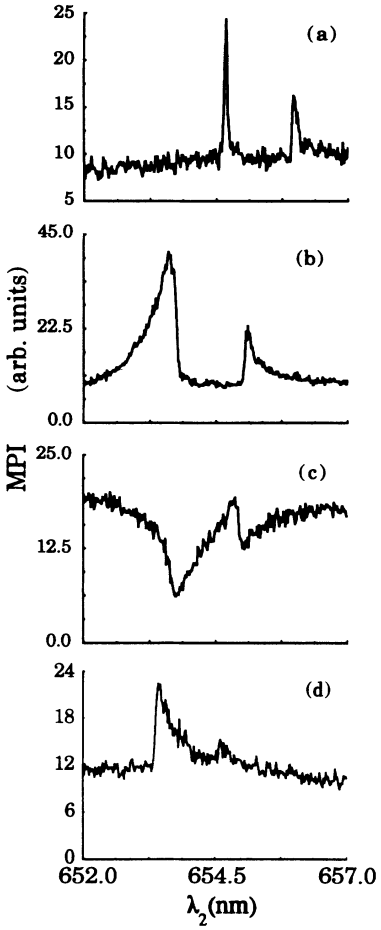

FIG. 7. Two-color MPI spectra dependence on the detuning $\Delta_1=E(3d4f\ ^1P_1)-3\hbar\omega_1$; $\Delta_1=23.0$ (a), 2.0 (b), $\simeq 0.0$ (c), and $-8.1\ \mathrm{cm}^{-1}$ (d). The asymmetric laser-induced peak turns to a dip for near-zero detuning.

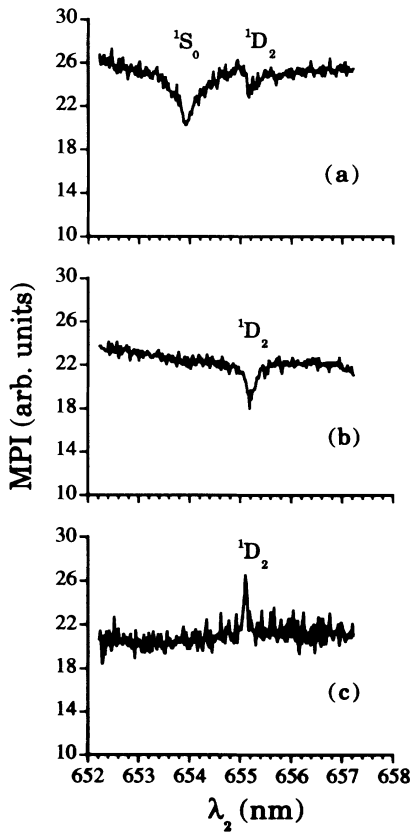

FIG. 8. Two-color MPI spectra as a function of ω_2 with $3\omega_1$ fixed so as to couple the $3d4f\ ^1P_1$ AIS with the ground state using parallel plane polarizations (a), crossed plane polarizations (b), and ω_1 circularly and ω_2 linearly polarized (c). In (b) the $4s6s\ ^1S_0$ cannot contribute to the coupling process, while in (c) the AIS cannot be excited from the ground state and only the $J=3$ continuum participates in the ionization process.

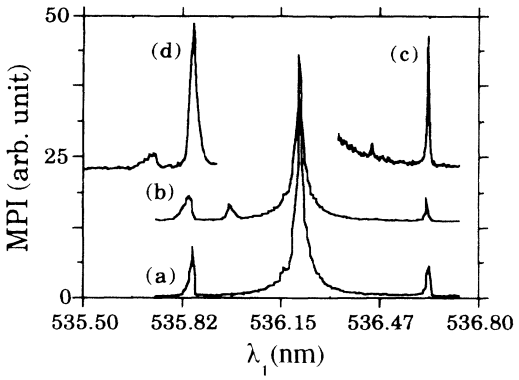

FIG. 9. One-color (a), two-color (b), and (c) and (d) MPI effusive beam spectra scanning frequency ω_1. ω_2 is fixed so as to couple the $4s6s\ ^1S_0$ bound state with the continuum between the $^1P_1$ and $^3P_1$ AIS's (b), between the $^3P_1$ and $^3D_1$ AIS's (c), and above the $^1P_1$ AIS.

10(a). The strong single-photon coupling of the $^1S_0$ state with the $^1P_1$ AIS results in an ac Stark splitting of the dressed AIS, or equivalently of the bound state. The two peaks observed correspond to the two Autler-Townes components of the split state probed by the field ω_1. The minimum between them is the result of the splitting itself but also of the destructive interference caused by the two components. The 7.5-cm^{-1} splitting has been observed

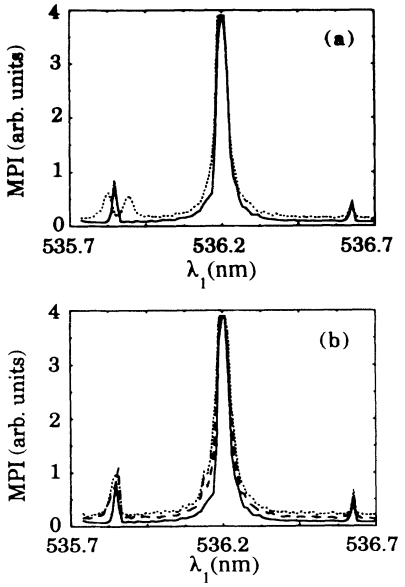

FIG. 10. MPI spectra as a function of ω_1 without (full line) and with (dotted line) the laser field ω_2 coupling the $4s6s\ ^1S_0$ (a) or $4p^2\ ^1D_2$ (b) bound states with the $3d4f\ ^1P_1$ AIS. In the first case an ac Stark splitting can clearly be seen due to the single-photon coupling, whereas in the second case the observed peak is only broadened. In (b), the curve plotted with the dashed line corresponds to a laser II intensity four times smaller than the curve plotted as a dotted line.

for $I_2 = 10^9$ W/cm^2. For the $4p^2\ ^1D_2$ state, however, no splitting has been observed for I_2 up to 4×10^9 W/cm^2. This is shown in Fig. 10(b) where the $^1P_1$ resonance is only broadened in the presence of ω_2, indicating that the $^1S_0$ is more efficiently coupled to the $^1P_1$ AIS than the $^1D_2$ state.

IV. DISCUSSION

The following is a discussion of the experimental results in developing an intuitive picture. It should be pointed out that there are several interconnected processes, occurring simultaneously and contributing to the observed structures, which may hinder such a formulation. The different shapes of the induced structures observed in our experiment at different laser intensities have been obtained theoretically through time-dependent density-matrix calculations, with calculated atomic parameters [16].

As already discussed in previous publications [12], the asymmetric line shapes and the window resonance dip observed can be understood if one makes the parallel between autoionization and LICS. By doing so the shape can be interpreted as being the result of a small near-zero q parameter value [2,3]. This is provided by a weak bound-bound coupling; that is, the overall two-photon Raman coupling between states $|2\rangle$ and $|3\rangle$ (Fig. 2). Such a weak bound-bound coupling is supported by the presence of the AIS state $|4\rangle$. This state resonantly enhances the strength of the Raman process having a pole in the continuum, which is commonly much weaker than the Raman process through the discrete part of the spectrum [3] for a structureless continuum. By making the amplitudes of the two Raman processes comparable and opposite in sign, their interference leads to a cancellation which minimizes the overall bound-bound coupling. The sign changes going over the AIS, which also may account for the asymmetry reversal in Fig. 7. It should be pointed out that there is a specific case in which the overall Raman coupling strength becomes practically zero. That is when both Raman processes as well as the excitation of the AIS are diminished due to ac Stark splitting of the bound state $|3\rangle$ and the $|4\rangle$ AIS, that may result from their strong single-photon coupling. Considering a symmetric splitting of the $|4\rangle$ AIS, and $3\omega_1$ being on resonance with the unsplit AIS, both the bound-bound coupling (the Raman processes) and the excitation of the AIS are diminished due to the splitting. This can easily be demonstrated in a dressed-atom picture. For the sake of simplicity let us first consider that field ω_2 is dressing the atom, whereas ω_1 is a probe. The coupling of the dressed state with the two Autler-Townes components corresponds to the two Raman couplings and the excitation of the AIS in the bare-atom picture. It is clear that the strength of these couplings becomes very small due to the destructure interference resulting from the opposite detunings of the two Autler-Townes components of each split dressed state, apart from the fact that due to the splitting we are dealing with a "near-resonance" but not "on-resonance" case. In the case of an asymmetric splitting due to an asymmetric AIS, there

is always a position (detuning) between the split components for which the destructive interference occurs. This effect may at least contribute to the dip observed when the $^1P_1$ AIS is coupled with the ^1S state, since the ac Stark splitting has been confirmed for this state when ω_2 is kept fixed and ω_1 is scanned. We would like to point out that the ac Stark splitting argument used here is very closely related to those of Boller, Imamoglu, and Harris [18] and Harris, Field, and Kasapi [19] in their works concerning laser-induced transparency. Since field ω_1 has an intensity comparable to field ω_2 and there are single-photon near-resonances involved, in the scheme investigated the simplified picture described above is not complete. Including dressing due to the field ω_2 and single-photon near-resonances, one additionally obtains ac Stark shifting of the states. In this dressed picture, minimization of the bound-bound coupling and hence of the effective q parameter is incorporated in the interference of the decay of the two shifted Autler-Townes components. The laser power density dependence of the observed laser-induced structure can be traced to the dependence of the widths, splitting, and positions of the states involved on the strength of the laser field. Thus the change of the LICS shape with the intensity of field ω_2 (Fig. 5) can be interpreted by means of an altered splitting or broadening of the bound and AIS states coupled with this field. Variation of the intensity of laser I would result in different shifts of the AIS caused by near-resonant single-photon couplings of the AIS with the bound states discussed above. Different shifts in turn lead to different detunings in the couplings of the states via ω_2. This would alter the cancellation conditions of the two Raman processes discussed above, as well the two Autler-Townes components in terms of their positions and mixed character. In both cases the result is an altered effective q parameter as well as an altered position of the near-resonant states, giving rise to a change of the asymmetry of the shape of the "Fano-like" structures. This interpretation is compatible with the spectra of Fig. 6. Similar changes of the LICS shapes could be induced by slightly changing the detuning of field ω_1, as discussed above (Fig. 7). The shifting of the states now is not due to the different intensity, but to the difference in the detuning.

Finally it is worth noting that in the spectra of the third-harmonic generation the shape of the induced structures will also depend on the phase-matching conditions, which are affected by the presence of the field ω_2. This laser-induced phase-matching effect has been reported recently [20].

V. CONCLUSION

In conclusion, a laser-induced continuum structure has been observed and experimentally investigated in a region of the continuum of atomic Ca which possesses structure, due to the presence of several AIS's. The effect under consideration has been studied in a heat-pipe environment, through observation of ionization or THG, as well as in an effusive atomic beam through ionization. Laser-induced "autoionizinglike" resonances have been observed in excitation spectra when the "inducing" laser frequence was detuned from the AIS. Modification of the AIS's, resulting from their coherent coupling with bound states, leads to the observation of induced structures in both the ionization and THG spectra, the shapes of which turn to be dependent on laser intensity and detuning, varying from window resonance dips to strongly asymmetric or less asymmetric peaks. The significant role of the AIS in the shape behavior of the induced structures has been verified through measurement with different beam polarizations. The effusive beam results have shown that the variable shape of the induced structures cannot simply be attributed to phase-matching effects and consequent reabsorption of the THG that leads to ionization. The experimental results have been discussed qualitatively by means of interfering excitation channels. It has been pointed out that ac Stark splitting due to strong single-photon couplings, and ac Stark shifting due to the presence of near-lying atomic resonances may play a dominant role in the above-mentioned interferences, and thus govern the shape of the laser-induced structures. Such ac Stark splitting has been demonstrated for one of the cases investigated.

ACKNOWLEDGMENT

This work has been carried out in the Ultraviolet Laser Facility operating at FORTH-IESL with support from the HCM Program (Contract No. ERB-CHGE-CT920007) of the European Union.

[1] J. M. Blatt and V. F. Weisskopf, *Theoretical Nuclear Physics* (Wiley, New York, 1952), p. 401.
[2] U. Fano, Phys. Rev. **124**, 1866 (1961).
[3] Bo-nian Dai and P. Lambropoulos, Phys. Rev. A **36**, 5205 (1987).
[4] V. G. Arkhipkin and Yu. I. Heller, Phys. Lett. **98A**, 12 (1983).
[5] S. E. Harris, Phys. Rev. Lett. **62**, 1033 (1989).
[6] Yu. I. Heller, V. F. Lukinykh, A. K. Popov, and V. V Slabko, Phys. Lett. A **82**, 4 (1981).
[7] L. I. Pavlov, S. S. Dimov, D. I. Metchkov, G. M. Mileva, and K. V. Stamenov, Phys. Lett. A **89**, 441 (1982).
[8] S. S. Dimov, L. I. Pavlov, and K. V. Stamenov, Appl. Phys. B **30**, 35 (1983).
[9] D. Feldmann, G. Otto, D. Petring, and K. H. Welge, J. Phys. B **19**, 269 (1986).
[10] M. H. R. Hutchinson and K. M. M. Ness, Phys. Rev. Lett. **60**, 105 (1988).
[11] S. Cavalieri, F. S. Pavone, and M. Matera, Phys. Rev. Lett. **67**, 3673 (1991).
[12] Y. L. Shao, D. Charalambidis, C. Fotakis, Jian Zhang, and P. Lambropoulos, Phys. Rev. Lett. **67**, 3669 (1991).
[13] S. Cavalieri, M. Matera, F. S. Pavone, Jian Zhang, P. Lambropoulos, and T. Nakajima, Phys. Rev. A **47**, 4219 (1993).
[14] P. L. Knight, M. A. Lauder, and B. J. Dalton, Phys. Rep. **190**, 1 (1990).
[15] O. Faucher, Y. L. Shao, and D. Charalambidis, J. Phys. B **26**, L309 (1993).
[16] O. Faucher, D. Charalambidis, C. Fotakis, Jian Zhang, and P. Lambropoulos, Phys. Rev. Lett. **70**, 3004 (1993).
[17] G. C. Bjorklund, IEEE J. Quantum Electron. **QE-11**, 287

(1975).
[18] K.-J. Boller, A. Imamoglu, and S. E. Harris, Phys. Rev. Lett. **66**, 2593 (1991).
[19] S. E. Harris, J. E. Field, and A. Kasapi, Phys. Rev. A **46**, R29 (1992).
[20] Maneesh Jain, G. Y. Yin, J. E. Field, and S. E. Harris, Opt. Lett. **18**, 998 (1993).